

Interaction of Chromium(II) Complexes with Molecular Oxygen. Spectroscopic and Kinetic Evidence for η^1 -Superoxo Complex Formation

Andreja Bakac,^{*,†} Susannah L. Scott,^{†,§} James H. Espenson,^{*,†} and Kenton R. Rodgers^{*,‡}

Contribution from the Departments of Chemistry, Iowa State University, Ames, Iowa 50011, and North Dakota State University, Fargo, North Dakota 58105

Received February 18, 1995[®]

Abstract: Two chromium adducts with molecular oxygen, $(\text{H}_2\text{O})_5\text{CrO}_2^{2+}$ and $(\text{H}_2\text{O})(\text{cyclam})\text{CrO}_2^{2+}$ (cyclam = [14]-aneN₄ = 1,4,8,11-tetraazacyclotetradecane), have been investigated by UV resonance Raman and transient absorption spectroscopic methods. The Raman bands at 1166 and 503 cm^{-1} for $(\text{H}_2\text{O})_5\text{CrO}_2^{2+}$ are the first such data for an aqua-transition-metal-superoxo complex. These bands shift to 1098 and 491 cm^{-1} upon $^{18}\text{O}_2$ substitution and are assigned to the $\nu_{\text{O}-\text{O}}$ and $\nu_{\text{Cr}-\text{O}-\text{O}}$ [stretching] vibrations, respectively. The corresponding vibrations in $(\text{H}_2\text{O})(\text{cyclam})\text{CrO}_2^{2+}$ were observed at lower frequencies, 1134/1145 (doublet) and 489 cm^{-1} . Both complexes are photolabile upon UV irradiation, yielding the respective Cr(II) complexes and O_2 . The quantum yield for photohomolysis at 290 nm (LMCT) is greater than that at 245 nm (superoxide-based $\pi-\pi^*$ transition). These vibrational and transient absorption data are consistent with electronic and kinetic behavior of these complexes and support assignment of both species as η^1 (end-on) superoxo complexes of Cr(III). Effects of the macrocyclic cyclam ligand on Cr-O₂ and O-O bonding are discussed. The O-O bond dissociation energy in $(\text{H}_2\text{O})_5\text{CrO}_2^{2+}$ is comparable to that in $\text{O}_2^{\cdot-}$ (393 kJ/mol).

Introduction

Activation of molecular oxygen by transition-metal complexes usually involves the formation of an O_2 adduct with the catalytic complex. The coordination geometries of these adducts fall into three categories, η^1 (end-on), η^2 (side-on), or μ (bridging). Examples from all of these categories have been characterized structurally and spectroscopically for chelated transition-metal complexes.¹ The electronic properties of the O_2 ligand are not always clear due to variable influence of ligand-based π electrons and axial ligand fields on metal-oxygen bonding. Nevertheless, in the study of metal ion- O_2 adducts it can be useful to discuss the complexes in terms of the electronic configurations of the metal ion and the O_2 ligand.

The formal oxidation state of the coordinated O_2 , insofar as it is useful to define it, may be close to 0 (molecular oxygen), 1- (superoxide), or 2- (peroxide). Each state exhibits characteristic ranges of bond lengths and O-O bond stretching frequencies.² The O-O stretching frequency in superoxo ligands falls in the range of 1075–1195 cm^{-1} , near the frequency of 1108 cm^{-1} for $\text{K}[\text{O}_2]$ and 1138 for HO_2 .² This range of frequencies includes both end-on (1103 to 1195 cm^{-1}) and bridging (1075–1122 cm^{-1}) coordination geometries. Of the two known complexes with side-on superoxo ligands, one^{3a}

(superoxocopper(II) complex of a substituted tris(pyrazolyl)-borate) has a frequency of 1111 cm^{-1} , well within the superoxo range. The frequency of the other,^{3b} $\text{Co}^{\text{II}}(\eta^2-\text{O}_2)(\text{tris}(\text{pyrazolyl})\text{-borate})$, is 961 cm^{-1} , much lower than that of all the other superoxo complexes. It has been shown that the matrix-isolated superoxo complexes of Li^+ and Cs^+ are side-on complexes.⁴ Together, these data suggest that the O-O frequency is not necessarily an indicator of coordination geometry, but rather reflects the O-O bond order. It is clear that $\nu_{\text{O}-\text{O}}$ frequencies of >1100 cm^{-1} in transition-metal- O_2 adducts are typical for superoxo complexes, and probably quite representative of η^1 geometry, although side-on coordination may be a possibility in certain cases.

Peroxo complexes exhibit O-O frequencies in the range between 750 and 930 cm^{-1} (cf. 750 cm^{-1} for $\text{K}_2[\text{O}_2]$).² This range encompasses those for side-on (800–929 cm^{-1}) and bridging (790–844 cm^{-1}) modes of coordination.^{2,5} While coordination of O_2 is nearly always accompanied by its reduction, it is not clear that the O_2 ligand assumes discrete oxidation states in all complexes. This is evidenced in macrocyclic complexes by the ability to tune O-O stretching frequencies within the range for the corresponding oxidation state by adjusting the basicity of the axial ligand *trans* to O_2 .² In the absence of a *trans* axial ligand, superoxo and peroxo adducts of macrocyclic Co complexes tend to have high O-O stretching frequencies relative to ionic $\text{O}_2^{\cdot-}$,^{2b} suggesting that less than one electron is transferred to O_2 upon coordination to the metal ion.

[†] Iowa State University.

[§] Present address: Department of Chemistry, University of Ottawa, Ottawa, Ontario, Canada.

[‡] North Dakota State University.

[®] Abstract published in *Advance ACS Abstracts*, June 1, 1995.

(1) (a) Valentine, J. S.; McCandlish, E. In *Electron Transport and Oxygen Utilization*; Ho, C., Ed.; Elsevier: New York, 1982; pp 229–235. (b) Hall, M. B. In *Oxygen Complexes and Oxygen Activation by Transition Metals*; Martell, A. E., Wawyer, D. T., Eds.; Plenum: New York, 1988, pp 3–16. (c) Loehr T. M. *Ibid.*, pp 17–32. (d) Gubbelmann, M. G.; Williams, A. F. *Struct. Bonding* **1983**, 55, 1. (e) McLendon, G.; Pickens, S. R.; Martell, A. E. *Inorg. Chem.* **1977**, 16, 1551.

(2) (a) Nakamoto, K. *Coord. Chem. Rev.* **1990**, 112, 363. (b) Suzuki, M.; Ishiguro, T.; Kozuka, M.; Nakamoto, K. *Inorg. Chem.* **1981**, 20, 1993. (c) Drago, R. S.; Corden, B. B. *Acc. Chem. Res.* **1980**, 13, 353.

(3) (a) Fujisawa, K.; Tanaka, M.; Moro-oka, Y.; Kitajima, N. *J. Am. Chem. Soc.* **1994**, 116, 12079. (b) Egan, J. W.; Haggerty, B. S.; Rheingold, A. L.; Sendlinger, S. C.; Theopold, K. H. *J. Am. Chem. Soc.* **1990**, 112, 2445.

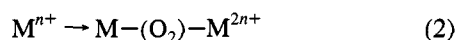
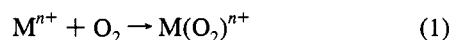
(4) Andrews, L. In *Cryochemistry*; Moskovits, M., Ozin, G., Eds.; John Wiley & Sons, Inc.: New York, 1976; Chapter 6, pp 195–230.

(5) (a) Vaska, L. *Acc. Chem. Res.* **1976**, 9, 175. (b) Feig, A. L.; Lippard, S. J. *Chem. Rev.* **1994**, 94, 759. (c) Kitajima, N.; Moro-oka, Y. *Chem. Rev.* **1994**, 94, 737. (d) Momenteau, M.; Reed, C. A. *Chem. Rev.* **1994**, 94, 659.

In order to design effective O₂-activation catalysts, it is beneficial to be able to distinguish M–O and O–O bonding properties that are intrinsic to the metal ion from those imposed on the complex by exogenous ligands. The complex (H₂O)₅CrO₂²⁺ is thermally and kinetically stable in dilute solution at 0 °C and provides an opportunity to study the electronic interactions and transitions involving only the O₂ ligand and the metal ion. Herein we present the results of a spectroscopic study of the adduct, (H₂O)₅CrO₂²⁺, and a macrocyclic analog, (H₂O)(cyclam)CrO₂²⁺ (cyclam = 1,4,8,11-tetraazacyclotetradecane). We have used UV resonance Raman (UVR) spectroscopy to probe the extent of electron transfer that occurs between the metal centers and O₂ in formation of these adducts. Comparison of UVR data from the two adducts reveals multidimensional influence of the macrocyclic ligand on Cr–O₂ and O–O bonding.

The reaction between Cr(H₂O)₆²⁺ and O₂ was discovered in 1913, when (HO)₂Cr(O₂)Cr(OH)₂, (HO)₂CrO, and (HO)₂CrO₂ were proposed as intermediates.⁶ The adduct (H₂O)₅CrO₂²⁺ was discovered in 1975 and was proposed to be a superoxochromium(III) complex⁷ on the basis of its electronic spectrum, which exhibits a 245-nm transition that is similar in energy and extinction coefficient to that of free superoxide ion (240 nm). The kinetic stability of the Cr–O₂ bond is characteristic of Cr(III) complexes in acidic solution, which are known to aquate very slowly.⁸ By contrast, O₂ adducts of chromium in other possible oxidation states would be expected to aquate rapidly, as Cr(II) and Cr(IV) are quite labile with respect to ligand substitution.⁹ Furthermore, it has been shown that thermal decomposition of the adduct involves rate-determining homolysis of the Cr–O₂ bond yielding Cr(H₂O)₆²⁺ and O₂.¹⁰ This process is electronically similar to the well-characterized homolysis of organochromium(III) complexes,¹¹ Cr(H₂O)₅R²⁺, and can only be observed because of slow and mechanistically distinct aquation of the Cr(III) center.

Structural characterization of monomeric transition-metal-ion adducts with O₂ is difficult because they often persist only in dilute solutions (<1 mM) due to their tendency to form peroxo-bridged binuclear complexes, as illustrated by eqs 1 and 2.



Frequencies of the M–O and O–O stretching vibrations can provide key insight into the bond strengths but, due to the necessity of working in dilute solutions, high sensitivity is needed to observe the spectra. In this study, we exploit the resonance enhancement of Raman-active Cr–(O₂) and O–O vibrations accessible at the wavelength of the superoxide-based absorption of (H₂O)₅CrO₂²⁺ ($\lambda_{\max} = 245$ nm, $\epsilon_{\max} = 7.4 \times 10^3$ M⁻¹ cm⁻¹) by using UV laser excitation. We have obtained vibrational frequencies of the coordinated O₂ ligand in both (H₂O)₅CrO₂²⁺ and the macrocyclic (H₂O)(cyclam)CrO₂²⁺ complex by this method. Since Raman scattering by the Cr(III) species arising from degradation of the adducts is not enhanced at our excitation wavelength, this experiment is blind to the inevitable Cr(III) impurities and interpretation of the spectra

(6) Piccard, J. *Ber. Dtsch. Chem. Ges.* **1913**, *46*, 2477.

(7) Sellers, R. M.; Simic, M. G. *J. Chem. Soc., Chem. Commun.* **1975**, 401.

(8) Hunt, J. P.; Taube, H. *J. Chem. Phys.* **1951**, *19*, 602.

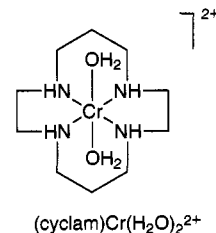
(9) Wilkins, R. G. *The Study of Kinetics and Mechanisms of Reactions of Transition Metal Complexes*; Allyn and Bacon: Boston, MA, 1974.

(10) Brynildson, M. E.; Bakac, A.; Espenson, J. H. *J. Am. Chem. Soc.* **1987**, *109*, 4579.

(11) Espenson, J. H. *Acc. Chem. Res.* **1992**, *25*, 222.

does not suffer from complications associated with these impurities. As far as we are aware, these are the first vibrational data for an aqua-transition-metal-ion–O₂ adduct. Also presented are transient absorption data, which confirm the photolysis of (H₂O)₅CrO₂²⁺ upon UV irradiation. These data support assignment of (H₂O)₅CrO₂²⁺ as a superoxochromium(III) complex and support the previous assignment of the 290-nm absorption as a ligand-to-metal charge-transfer (LMCT) transition.⁷

Even though the extent of water coordination has not been determined for either complex, we believe that the formulas (H₂O)₅CrO₂²⁺ and (cyclam)(H₂O)CrO₂²⁺ are likely. As shown in this work, these are η^1 -superoxo complexes of Cr(III), and therefore, most likely, hexacoordinate. The abbreviated notation, CrO₂²⁺ and (cyclam)CrO₂²⁺, will be used hereafter.



Experimental Methods

Preparation of Starting Materials. Solutions of Cr²⁺ were prepared by dissolving a weighed amount of electrolytic Cr metal in 4 M HCl or HClO₄ under a constant stream of N₂. Solutions containing HClO₄ were treated with Zn/Hg to reduce trace amounts of Cr³⁺. Na₂Cr₂O₇, H₂O₂, and CH₃OH were obtained from commercial sources and used without further purification. The preparation of [Cr(cyclam)(H₂O)₂](CF₃SO₃)₃ was reported previously.¹²

Preparation of Molecular Oxygen Adducts. Solutions of CrO₂²⁺ were prepared by two different methods. The first is the reaction between Cr²⁺ and O₂ in aqueous acidic solution.^{7,13} One milliliter of 6.7 mM Cr²⁺ was injected into 20 mL of ice-cold, O₂-saturated 0.02 M HClO₄ containing 0.035 M CH₃OH (total [Cr] = 0.35 mM). The UV absorption spectrum contained two peaks with λ_{\max} at 290 and 245 nm. The concentration of CrO₂²⁺ was calculated to be 0.31 mM using the published extinction coefficients, $\epsilon_{290} = 3100$ M⁻¹ cm⁻¹ and $\epsilon_{245} = 7400$ M⁻¹ cm⁻¹.¹³

The second method is based on the reaction of Cr(VI) with H₂O₂.¹⁴ The yield of this reaction is strongly acid-dependent, requiring 0.1 M H₃O⁺ to generate useful concentrations of CrO₂²⁺. To avoid having the UVR spectra dominated by the symmetric ClO₄⁻ stretch at 935 cm⁻¹, the reaction was carried out in solutions that were 0.02 M in HClO₄ and 0.08 M in HCl. The CrO₂²⁺ solution was prepared by injecting 0.3 mL of 7.5 mM Cr(VI) into 2.7 mL of a solution that was 0.02 M in HClO₄, 0.08 M in HCl, and 7.6 mM in H₂O₂. The blue color of CrO(O₂)₂ (oxodiperoxochromium(VI)) appeared immediately, then faded over the next few minutes to give a colorless solution of CrO₂²⁺ in 32% yield. The reaction mixture was then saturated with O₂ in an ice/water bath. The CrO₂²⁺ concentration was determined to be 0.24 mM on the basis of the 290- and 245-nm absorbances. The UVR spectrum of CrO₂²⁺ prepared by this method was identical to that obtained from the compound prepared by direct reaction of Cr²⁺ and O₂. Samples were kept in ice and used within 2 to 3 h, after which they showed significant decomposition.¹⁰

(cyclam)CrO₂²⁺ was prepared¹⁵ in solution by reducing 5.4 mM Cr(cyclam)³⁺ in 0.02 M HClO₄ over Zn/Hg until the color change from pink (Cr^{III}) to red (Cr^{II}) was complete (about 5 min with N₂ bubbling through the solution). The O₂ adduct was generated by injecting 0.75 mL of the Cr(cyclam)²⁺ solution into 20 mL of ice-

(12) Bakac, A.; Espenson, J. H. *Inorg. Chem.* **1992**, *31*, 1108.

(13) (a) Ilan, Y. A.; Czapski, G.; Ardon, M. *Isr. J. Chem.* **1975**, *13*, 15.

(b) Sellers, R. M.; Simic, M. G. *J. Am. Chem. Soc.* **1976**, *98*, 6145.

(14) Al-Ajlouni, A.; Espenson, J. H.; Bakac, A. *Inorg. Chem.* **1993**, *32*, 3162.

(15) Bakac, A. Unpublished observations.

cold, O₂-saturated 0.02 M HClO₄. The solution was resaturated with O₂, after which the addition of Cr(cyclam)²⁺ was repeated. The concentration of (cyclam)CrO₂²⁺ was calculated to be 0.18 mM on the basis of the 290-nm absorbance ($\epsilon_{290} = 2700 \text{ M}^{-1} \text{ cm}^{-1}$),¹⁵ corresponding to a 48% yield. This solution was frozen and used over the course of the next 2 days.

Resonance Raman Spectroscopy. Samples were contained in a 5-mm Suprasil NMR tube which was spun at approximately 20 Hz in a stream of cold N₂ (liquid-N₂ boiloff). The NMR tube was spun around a stationary Teflon-coated helical wire to affect vertical mixing of the sample solution.^{16,17} The sample temperature was maintained near 0 °C; samples were not allowed to freeze. Ultraviolet Raman excitation wavelengths (290 and 245 nm) were generated with a frequency-doubled dye laser pumped by a XeCl-excimer laser. Laser pulse widths in the UV were 6–7 ns. The laser was run at a repetition rate of 300 Hz and the average power was typically 3 mW. Scattered light was collected with a cassegrain collector, focused on the slit of a 1.27-m single spectrograph, and dispersed on an intensified 1024-diode array detector using a 3600-groove/mm holographic grating. Ethanol, acetone, dimethylformamide, and *n*-pentane were used as external frequency references for spectral calibration.

Transient Absorption Spectroscopy. Photolysis of CrO₂²⁺ in 0.10 M HClO₄ in the presence of excess O₂ was accomplished with the fourth harmonic (266 nm) of a Q-switched Nd:YAG laser.¹⁸ Recombination of the photolysis products was followed by monitoring the recovery of the absorbance at the 290-nm maximum of the CrO₂²⁺ absorption spectrum. Changes in absorption were monitored as a function of time and fitted to a single exponential function.

Results

Resonance Raman Spectroscopy of CrO₂²⁺. Raman excitation of CrO₂²⁺ and the ¹⁸O₂ analog at 245 nm yielded the RR spectra in Figure 1. The 245-nm absorption of CrO₂²⁺ has been tentatively assigned to a superoxide-based $\pi-\pi^*$ electronic transition by comparison with the UV absorption spectrum of free superoxide ion, which exhibits a single peak at 240 nm.¹⁹ This transition corresponds to a lowering of the O–O bond order and, therefore, displacement of the equilibrium positions of the oxygen atoms in the excited state along the ground-state O–O stretching coordinate. Hence, Raman excitation at the energy of this transition is expected to resonance enhance Raman scattering by the O–O stretching mode.²⁰ Raman modes that are not resonance enhanced would be undetectable with our spectrometer at submillimolar concentrations of CrO₂²⁺. As seen in Figure 1, the UVRR spectra reveal two resonance-enhanced modes. On the basis of the isotope shifts, the band at 1166 cm⁻¹ in the natural-abundance spectrum is assigned to the O–O stretching vibration and that at 502 cm⁻¹ to the Cr–O₂ stretch. The frequency of the 1166-cm⁻¹ band lies toward the high end of the range that is diagnostic for end-on O₂ coordination to six-coordinate macrocyclic Fe(II) and Co(II) complexes.² The 502-cm⁻¹ band also falls within the known range of M–O₂ stretching frequencies for η^1 -coordination of O₂ to Fe(II) and Co(II) complexes.² The simultaneous enhancement of the Cr–O₂ stretch with 245-nm excitation (Figure 1) shows that the excited-state distortion of CrO₂²⁺ also involves atomic displacement along the Cr–O₂ coordinate. Such a distortion could be rationalized in terms of either the end-on or the side-on bonding geometry. The spectrum of a side-on

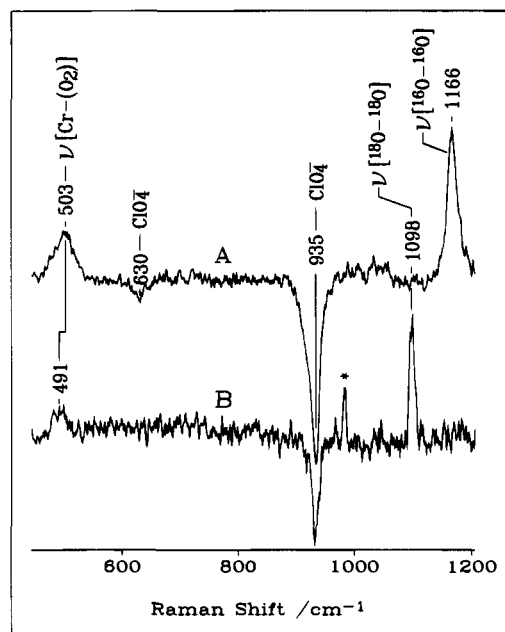


Figure 1. 245-nm excited resonance Raman spectra of (A) 0.225 mM CrO₂²⁺ and (B) $\sim 50 \mu\text{M}$ Cr¹⁸O₂²⁺ in 0.02 M HClO₄ at 0 °C. Average laser power was 3 mW at the shot frequency of 300 Hz. Negative peaks arise from subtraction of the aqueous HClO₄ spectrum in which the perchlorate bands at 934 and 629 cm⁻¹ were more intense. The subtraction procedure was carried out to remove the quartz bands from the CrO₂²⁺ spectra. The asterisk indicates a burned spot on the intensifier of the diode-array detector.

complex would be expected to exhibit both symmetric and asymmetric Cr–O₂ stretches, as both vibrations are Raman active for molecules with C_{2v} symmetry. However, since the asymmetric stretch is a non-totally symmetric vibration under C_{2v} symmetry, it will not gain resonance enhancement by A-term scattering with 245-nm excitation. Thus, it is unlikely that we would observe the asymmetric stretch of a side-on O₂ complex at the submillimolar concentrations used in these experiments. Nevertheless, our observation of the 502-cm⁻¹ Cr–O₂ stretch and the 1166-cm⁻¹ O–O stretch is consistent with the end-on geometry.

Both bands in the RR spectrum of CrO₂²⁺ showed a parallel loss of intensity upon exposure to the UV laser beam for 1 min. The intensity loss was accelerated by decreasing the sample spinning rate and by increasing the laser power. Vertical repositioning of the sample in the laser beam resulted in reappearance of the RR spectrum in Figure 1. Since vertical mixing is inefficient in a spinning tube,^{16,17} we placed a stationary helical stirring wire in the spinning tube to affect vertical mixing of the sample. This resulted in a sample lifetime in the laser beam of several minutes. The spectra in Figures 1–3 were obtained by adding the spectra from three to five samples. These observations indicate that loss of Raman intensity is due to photolysis of the CrO₂²⁺ complex in the laser beam.

The 290-nm absorption of CrO₂²⁺ has been attributed to a LMCT transition, as there is no such absorption in the spectrum of superoxide ion, and the extinction coefficient at 290 nm, 3100 M⁻¹ cm⁻¹, is too large for a Cr-based d–d transition. Attempts to acquire RR spectra by exciting at the maximum of the 290-nm LMCT absorption resulted in spectra containing only bands from the perchlorate ion. No bands attributable to CrO₂²⁺ were observed, regardless of the laser power used. This suggested that 290-nm irradiation results in photolytic cleavage of the Cr–(O₂) bond with higher quantum yield than that observed at 245

(16) Rodgers, K. R.; Su, C.; Subramaniam, S.; Spiro, T. G. *J. Am. Chem. Soc.* **1992**, *114*, 3697.

(17) Austin, J. C.; Rodgers, K. R.; Spiro, T. G. *Methods Enzymol.* **1993**, *226*, 374.

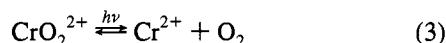
(18) Huston, P.; Espenson, J. H.; Bakac, A. *J. Am. Chem. Soc.* **1992**, *114*, 9510.

(19) Bielski, B. H. *Photochem. Photobiol.* **1978**, *28*, 645.

(20) Myers, A.; Mathies, R. A. In *Biological Applications of Raman Spectroscopy*; Spiro, T. G., Ed.; John Wiley & Sons, Inc.: New York, 1987; Vol. 2, pp 1–58.

nm. It may be that the photolysis observed with 245-nm excitation results from the small contribution of the 290-nm absorption (LMCT) band to ϵ_{245} . This would explain the increased efficiency of photolysis at 290 nm in spite of its smaller extinction coefficient and the lack of any O_2 bands in the UVRR spectra. Owing to this wavelength-dependent photodegradation, it was not possible to record a meaningful excitation profile.

A reasonable mechanism for this process is the photoinduced homolytic cleavage of the Cr-(O_2) bond followed by trapping of the resultant Cr^{2+} by CrO_2^{2+} , as illustrated in eqs 3 and 4.



This photodecomposition scheme parallels the established thermal decomposition reactions of CrO_2^{2+} .¹⁰

Transient Absorption of Photolyzed CrO_2^{2+} . The photochemistry described above was investigated and confirmed by optical pump and probe transient absorption experiments. Photolysis of CrO_2^{2+} in 0.10 M $HClO_4$ with a 10-ns 266-nm laser flash resulted in bleaching of the 245- and 290-nm absorptions. The absorbance then increased in a subsequent slower process characterized by $[O_2]$ - and $[CrO_2^{2+}]$ -dependent kinetics. We interpret these observations as a photoinduced homolytic cleavage of the Cr- O_2 bond, followed by thermal recombination of the photolysis products.

Consistent with eqs 3 and 4, the extent of CrO_2^{2+} recovery and the values of pseudo-first-order constants are a function of $[CrO_2^{2+}]$ and $[O_2]$, eq 5.

$$-d[Cr^{2+}]/dt = k_{obs}[Cr^{2+}] = (k_{-3}[O_2] + k_4[CrO_2^{2+}])[Cr^{2+}] \quad (5)$$

At low $[CrO_2^{2+}]$ and/or low $[O_2]$, the signal-to-noise ratio was small, and only an approximate value of the rate constant could be obtained, $k_{-3} \sim 10^8 \text{ M}^{-1} \text{ s}^{-1}$, in reasonable agreement with the published value of $(1.6 \pm 0.2) \times 10^8 \text{ M}^{-1} \text{ s}^{-1}$.¹³ In an experiment at much higher concentrations, $[CrO_2^{2+}] = 1.4 \times 10^{-4} \text{ M}$ and $[O_2] = 1.27 \times 10^{-3} \text{ M}$, only 60% of the photolyzed CrO_2^{2+} was recovered after the flash. The measured rate constant was $3.3 \times 10^5 \text{ s}^{-1}$. These data are in excellent agreement with the predicted 62% recovery and $k_{5(calc)} = 3.4 \times 10^5 \text{ s}^{-1}$ on the basis of published values for k_{-3} ($1.6 \times 10^8 \text{ M}^{-1} \text{ s}^{-1}$)¹³ and k_4 ($8 \times 10^8 \text{ M}^{-1} \text{ s}^{-1}$).¹⁰ We are thus confident the photoinduced reaction takes place as in eqs 3 and 4.

Resonance Raman Spectroscopy of (cyclam) CrO_2^{2+} . The electronic spectrum of (cyclam) CrO_2^{2+} contains several weak bands in the visible region and an intense band at 290 nm. As was the case for CrO_2^{2+} , Raman excitation of (cyclam) CrO_2^{2+} at 290 nm did not yield any Raman bands attributable to the O-O stretching vibration. Although an electronic absorption band associated with the cyclam ligand overlaps the (presumably) superoxide-based transition, there is a discernible shoulder at approximately 245 nm. Raman excitation at this wavelength yielded the RR spectrum in Figure 2A. Most of the Raman bands arise from the cyclam ligand, as demonstrated by the 245-nm excited RR spectrum of $Cr(\text{cyclam})^{3+}$ in Figure 2B. Nevertheless, bands attributable to the O-O and Cr- O_2 stretching vibrations are present in the spectrum of (cyclam)- CrO_2^{2+} at 1134, 1145, and 489 cm^{-1} . As with CrO_2^{2+} , the intensity of the bands associated with the O_2 complex decreased in intensity within minutes of exposure to the UV laser beam

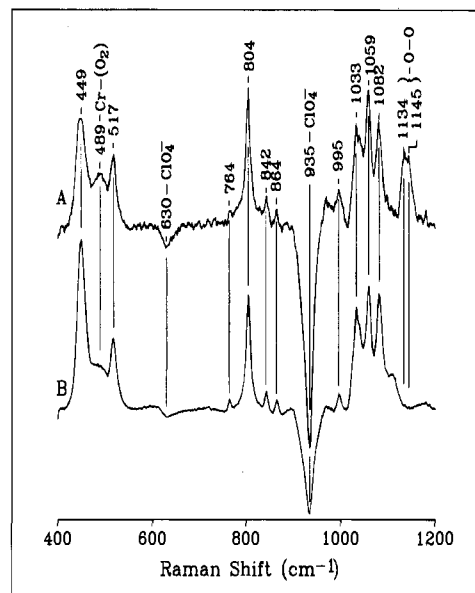


Figure 2. 245-nm excited resonance Raman spectra (taken at 0 °C) of (A) 0.18 mM (cyclam) CrO_2^{2+} in 0.02 M $HClO_4$. Average laser power was 3 mW at the shot frequency of 300 Hz. Bands labeled only with frequencies arise from cyclam ligand modes as judged by their presence in (B), the spectrum of 5.4 mM $Cr(\text{cyclam})^{3+}$. Negative peaks result from subtraction of the aqueous $HClO_4$ spectrum to remove quartz bands from the spectra.

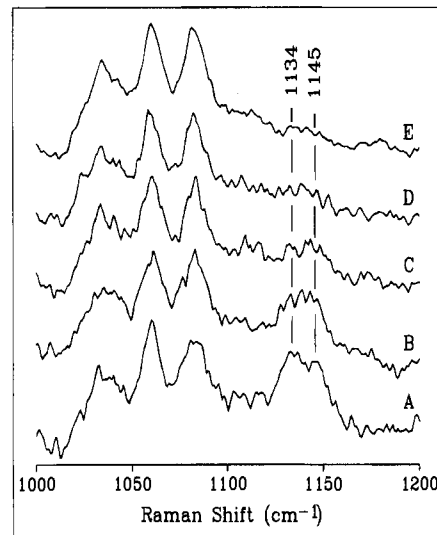


Figure 3. A series of 245-nm excited resonance Raman spectra of 0.26 mM (cyclam) CrO_2^{2+} depicting the decrease in intensity of the 1134/1145- cm^{-1} O-O stretching bands with continuing exposure to the UV laser beam. Spectra A through E represent sequential 1.5-min spectral acquisitions using the same stirred sample. Average laser power was 3 mW at the shot frequency of 300 Hz.

(Figure 3), indicating a photodegradation process similar to that of CrO_2^{2+} . On the basis of the same arguments presented for CrO_2^{2+} , we conclude that the 1134/1145- cm^{-1} doublet arises from the O-O stretch of a terminally bound O_2 ligand. Although it is less clear for the cyclam complex than for the aqua complex, at least some of the intensity at 489 cm^{-1} is attributable to the Cr- O_2 vibration, because the intensity decreases with exposure to the laser beam.

We also collected ESR and magnetic susceptibility data on CrO_2^{2+} solutions. Meaningful interpretation of these data was unavoidably complicated by the presence of the paramagnetic species generated by thermal and photoinduced decomposition.

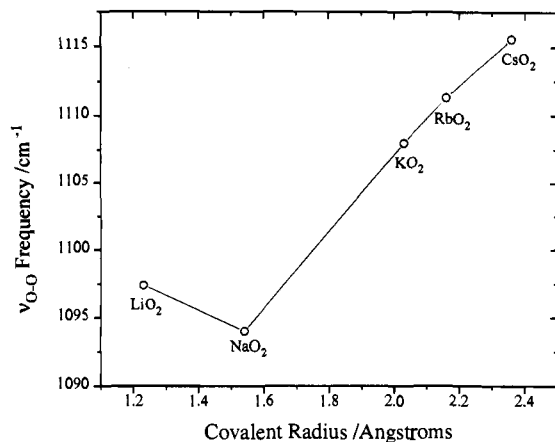


Figure 4. O—O stretching frequencies of matrix-isolated alkali metal superoxides versus covalent radius of the corresponding alkali metal ion. Data are from ref 4.

Discussion

The O—O bond. CrO_2^{2+} ion is the only aqua-transition-metal- O_2 adduct to be vibrationally characterized to date. Hence, this is the first system in which O_2 coordination to an aqua metal ion can be compared with that of a macrocyclic complex of the same metal ion. It has been argued that the frequency of the O—O stretching vibration ($\nu_{\text{O-O}}$) is a less-than-reliable indicator of the oxidation state of the bound O_2 ligand, because of its insensitivity to the covalency of the M—O bond.²¹ However, it has been shown that in matrix-isolated superoxides of alkali metals (i.e. isolated ionic superoxide-containing molecules), there is a correlation between the size of the metal ion and $\nu_{\text{O-O}}$, with $\nu_{\text{O-O}}$ increasing from 1094 to 1116 cm^{-1} in concert with the increasing covalent radius of the metal ion.⁴ This correlation is illustrated in Figure 4. The trend in these frequencies has been rationalized in terms of increasing cation polarization, which results in greater covalency in the case of larger and softer metal ions.⁴ The frequency of the Li^+ adduct is a clear outlier in the group. The anomalously high $\nu_{\text{O-O}}$ frequency for LiO_2 may be the consequence of slight Li-O_2 covalency arising from the extraordinary electron affinity of Li^+ . Consistent with this argument, the O—O stretching frequency for HO_2 , which contains a polar covalent H—O bond, is at 1138 cm^{-1} . Hence, the polar covalency of the H—O and Li—O bonds reduces the occupation of the superoxide-centered antibonding orbital. It is noteworthy that the differences between the O—O frequencies of KO_2 , RbO_2 , and CsO_2 are a measureable fraction of the difference between the CsO_2 and HO_2 frequencies. Hence, based on these data⁴ it would appear that the $\nu_{\text{O-O}}$ frequency is actually exquisitely sensitive to the covalency of the M—O bond. The extent of this sensitivity may be further appreciated by considering the dissociation energies and percent ionic character of alkali metal-halide bonds.²² Although these bond parameters are virtually indistinguishable by thermodynamic measurements^{22a} or model calculations,^{22b} the O—O frequencies of their superoxo complexes show a clear trend, as a function of metal ion covalent radius or polarizability (Figure 4). Furthermore, in simple vibrationally uncoupled diatomic oscillators, the vibrational frequency directly reflects the strength of the bond (magnitude of the force constant) between the atoms. If it can be shown that virtually all of the

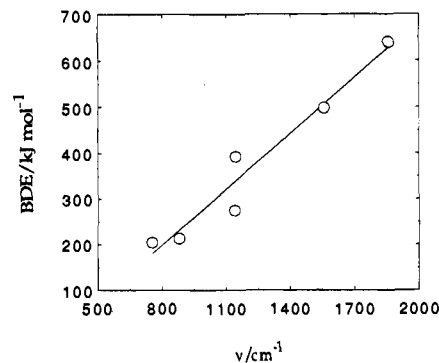


Figure 5. Correlation between gas-phase O—O bond energies and O—O stretching frequencies for O_2 species. In the order of increasing $\nu_{\text{O-O}}$, the data points are shown for O_2^{2-} , H_2O_2 , HO_2^\cdot , $\text{O}_2^{\cdot-}$, O_2 , and O_2^{2+} .

potential energy of the $\nu_{\text{O-O}}$ mode is associated with displacement of the oxygen atoms in CrO_2^{2+} , then the observed frequency is that of a pure O_2 oscillator and must relate directly to the strength of the O—O bond. One indicator of the purity of a diatomic vibration is the ability to predict its frequency shift in the spectrum of an isotopomer based on the assumption of a harmonic oscillator. This simple model leads us to predict a 68- cm^{-1} downshift, placing $\nu^{18\text{O}-18\text{O}}$ at 1098 cm^{-1} for $\text{Cr}^{18}\text{O}_2^{2+}$. Figure 1 reveals that the observed frequency corresponds exactly with that predicted using the diatomic harmonic oscillator model. Hence, the vibrational mode corresponding to the 1166- cm^{-1} band in our UVR spectrum of CrO_2^{2+} is an isolated O—O oscillator.

Having demonstrated the diatomic nature of the 1166- cm^{-1} vibration, we can estimate the O—O bond energy in CrO_2^{2+} . Figure 5 shows a plot of the bond dissociation energies (BDE) against the vibrational frequencies $\nu_{\text{O-O}}$ for $\text{O}_2^{\cdot+}$, O_2 , HO_2^\cdot , $\text{O}_2^{\cdot-}$, O_2^{2-} , and H_2O_2 . The BDE's for HO_2^\cdot and $\text{O}_2^{\cdot-}$ were calculated from the available thermodynamic data.^{23,24} Literature values were used for the remaining BDE's and for the vibrational frequencies.^{2,24,25} As shown in Figure 5, an approximately linear correlation exists between the two parameters. If we make a reasonable assumption that the data for CrO_2^{2+} would fall on the same line, then the value of BDE for the O—O bond is very close to that for $\text{O}_2^{\cdot-}$, 393 kJ/mol. This is, by definition, a gas-phase value. Thermodynamic data that would allow a similar comparison in aqueous solution are not available.

We believe that our results support the conclusion that the π^* occupancies of ionic $\text{O}_2^{\cdot-}$ and the coordinated $\text{O}_2^{\cdot-}$ are comparable. To put the difference between free and coordinated superoxide into other terms, our data indicate that in the formation of CrO_2^{2+} , the O_2 ligand is reduced by >0.9 electron relative to molecular oxygen. Application of Badger's rule²⁶ indicates that the bond length of the coordinated $\text{O}_2^{\cdot-}$ is only on the order of 0.02 Å shorter than that of ionic $\text{O}_2^{\cdot-}$ (1.28 Å).^{2,25} This difference is significantly less than those between ionic $\text{O}_2^{\cdot-}$ and either O_2 (-0.073 Å)²⁵ or O_2^{2-} (+0.21 Å).²⁵ Hence, our frequency data, being directly related to the bond length and bond energy, clearly support assignment of the O_2 ligand in CrO_2^{2+} as essentially a coordinated superoxide ion. Our conclusion is consistent with several established observa-

(23) Benson, S. W.; Nangia, P. S. *J. Am. Chem. Soc.* **1980**, *102*, 2843.

(24) *Standard Potentials in Aqueous Solution*; Bard, A. J., Parsons, R., Jordan, J., Eds.; Dekker: New York, 1985; Chapter 4.

(25) Jones, R. D.; Somerville, D. A.; Basolo, F. *Chem. Rev.* **1979**, *79*, 139.

(26) (a) Badger, R. M. *J. Chem. Phys.* **1934**, *2*, 128. (b) Badger, R. M. *J. Chem. Phys.* **1935**, *3*, 710. (c) Hershbach, D. R.; Laurie, V. W. *J. Chem. Phys.* **1961**, *5*, 458.

(21) (a) Tovrog, B. S.; Kitko, D. J.; Drago, R. S. *J. Am. Chem. Soc.* **1976**, *98*, 5144. (b) Drago, R. S. *Inorg. Chem.* **1979**, *18*, 1408. (c) Drago, R. S.; Corde, B. B.; Zombeck, A. *Comm. Inorg. Chem.* **1981**, *1*, 53.

(22) (a) Sanderson, R. T. *Chemical Bonds and Bond Energy*, 2nd ed.; Academic Press: New York, 1976. (b) Drago, R. S.; Wong, N.; Ferris, D. C. *J. Am. Chem. Soc.* **1991**, *113*, 1970.

tions that also argue for this assignment, namely the similarity between the 245-nm absorption of CrO_2^{2+} and that of free superoxide ion,¹⁹ the slow rate of O_2 dissociation from CrO_2^{2+} ,¹⁰ a property typical of aqueous Cr(III) complexes, and the superoxide-like reactivity of CrO_2^{2+} toward inner- and outer-sphere reducing agents.^{27,28}

The Cr–O Bond. In CrO_2^{2+} , the Cr–O stretching vibration, $\nu_{\text{Cr-O}}$, occurs at 503 cm^{-1} for the natural abundance adduct. This is consistent with frequencies observed for end-on O_2 adducts of macrocyclic and chelate complexes.² On the basis of a simple diatomic oscillator model, the predicted frequency of the $\nu_{\text{Cr-}^{18}\text{O}}$ vibration is 481 cm^{-1} . However, the spectrum of $\text{Cr}^{18}\text{O}_2^{2+}$ in Figure 1 shows that the frequency of this mode is at 491 cm^{-1} , corresponding to a 12-cm^{-1} downshift compared to the predicted 22-cm^{-1} shift. This discrepancy suggests that the reduced mass of the oscillator is actually larger than that of Cr–O. We, therefore, considered the possibility of an $\eta^2\text{-Cr-O}_2$ oscillator, which results in a predicted downshift of 19 cm^{-1} that is still significantly larger than the observed 12-cm^{-1} shift. These comparisons suggest that the 503-cm^{-1} mode is not a pure Cr–O oscillator. This is not surprising since all of the ligands in this complex are bonded to Cr through atoms of the same mass, namely oxygens. Hence, the discrepancy between the predicted and observed frequencies may be rationalized in terms of coupling between the Cr–O stretch and other internal coordinates such as the Cr–O–O bend, $\delta_{\text{Cr-O-O}}$, which has been observed in $\text{Fe}(\text{pc})(\text{O}_2)^{2-}$, and/or one or more $\text{Cr}(\text{OH}_2)$ vibrations. Nevertheless, it is clear from the frequency and the observed 12-cm^{-1} downshift of the 503-cm^{-1} mode with $^{18}\text{O}_2$ substitution that it has significant Cr–O stretching character.

(cyclam) CrO_2^{2+} . The 245-nm excited UVRR spectra of $\text{Cr}(\text{cyclam})^{3+}$ and $(\text{cyclam})\text{CrO}_2^{2+}$ are shown in Figure 2. The majority of the bands in these spectra no doubt correspond to cyclam-based modes, as evidenced by the similarity between the two spectra. The $(\text{cyclam})\text{CrO}_2^{2+}$ spectrum contains three new bands at 1145, 1134, and 489 cm^{-1} . By analogy to the aqua complex, we assign the 489-cm^{-1} band to a mode with Cr–O stretching character. Similarly, one or both components of the high-frequency doublet are assigned to O–O stretching vibrations. Both vibrations occur at lower frequencies than their counterparts in the aqua complex. This can be rationalized in two ways. First, there may be a slight increase in the extent of electron transfer from chromium to O_2 due to strong donation from the cyclam ligand, as evidenced by the lower reduction potential for the $\text{Cr}(\text{cyclam})^{3+/2+}$ couple ($E^\circ = -0.64\text{ V}$)²⁹ compared to the $\text{Cr}^{3+/2+}$ couple (-0.41 V). The increased electron transfer further populates O_2 -based antibonding orbitals, thereby decreasing the order of the O–O bond and, consequently, the frequency of the O–O stretching vibration. There is also a possibility of intramolecular hydrogen bonding between the terminal oxygen atom of the O_2 ligand and one or two NH protons of the macrocycle. Considerable thermodynamic and kinetic evidence exists for H-bond stabilization of coordinated O_2 in heme proteins and base-appended model hemes.² In

addition to stabilizing O_2 complexes, the H-bonds serve to decrease their O–O stretching frequencies.^{2,30}

The occurrence of two bands at 1134 and 1145 cm^{-1} can also be rationalized in terms of intramolecular H-bonding. These bands may reflect disorder in the status of H-bonding between the terminal oxygen atom and the amine protons of the cyclam ligand. The $\nu_{\text{O-O}}$ doublet is consistent with a double-well potential with minimum-energy conformations having single and bifurcated H-bonds with adjacent NH protons on the same side of the cyclam N_4 plane. The distance from the nitrogen to the terminal oxygen atom of the coordinated superoxide was estimated by means of a molecular mechanics calculation and is favorable for H-bond formation in both of these conformations (2.9 and 2.3 Å). This would give rise to two $\nu_{\text{O-O}}$ frequencies, both of which would be lower than that for a non-hydrogen-bonded superoxide ligand.

If hydrogen bonding is indeed responsible, then it is surprising that the spectrum of CrO_2^{2+} does not exhibit a similar doublet. In principle, hydrogen bonding between coordinated $\text{O}_2^{\cdot-}$ and *cis*-water molecules appears feasible. Possibly, the rigidity of ligand structure in $(\text{cyclam})\text{CrO}_2^{2+}$ can account for the differences in hydrogen bonding pattern and/or the spectra of the two superoxo complexes.

The doublet also could be rationalized on the basis of vibrational coupling between the O–O stretch and a cyclam-based mode whose scattering is not normally resonance enhanced by 245-nm Raman excitation. This is, however, less likely, because such coupling in metalloporphyrin- O_2 adducts^{2,31} occurs primarily with trans axial ligands and solvent molecules.

Conclusion

The UVRR and transient absorption data indicate that the product of the reaction between Cr^{2+} and O_2 is an η^1 -superoxochromium(III) complex. The Cr– O_2 bond is quite photolabile at wavelengths near the maximum of the 290-nm LMCT transition. The immediate photoproducts are the starting materials, Cr^{2+} and O_2 , which undergo thermal recombination in competition with reduction of unphotolyzed CrO_2^{2+} by Cr^{2+} to yield Cr(III) complexes. The ability to obtain vibrational data of these adducts has allowed us to compare the Cr–O and O–O bonding in the aqua complex with that in a macrocyclic complex of the same metal ion. The cyclam ligand has the effect of lowering the Cr– O_2 and O–O stretching frequencies, suggesting a decrease in these bond energies.

Acknowledgment. This work was supported by a grant from the National Science Foundation (CHE-9007283). Some of the experiments were conducted with the use of the facilities of the Ames Laboratory. The authors express their gratitude to professor Thomas G. Spiro for the use of his UV Raman spectrometer (Grant No. GM52158) and for his helpful comments during the preparation of this manuscript.

JA950427J

(27) Bakac, A. *Prog. Inorg. Chem.* In press.

(28) (a) Bruhn, S. L.; Bakac, A.; Espenson, J. H. *Inorg. Chem.* **1986**, *25*, 535. (b) Brynildson, M. E.; Bakac, A.; Espenson, J. H. *Inorg. Chem.* **1988**, *27*, 2592.

(29) (a) Bakac, A.; Butkovic, V.; Espenson, J. H.; Orhanovic, O. *Inorg. Chem.* **1993**, *32*, 5886. (b) Guldi, D.; Wasgestian, F.; Zeigerson, E.; Meyerstein, D. *Inorg. Chim. Acta* **1991**, *182*, 131.

(30) (a) Tsubaki, M.; Yu, N.-T. *Proc. Natl. Acad. Sci. U.S.A.* **1981**, *78*, 3581. (b) Kitagawa, T.; Ondrias, M. R.; Rousseau, D. L.; Ikeda-Saito, M.; Yonetani, T. *Nature* **1982**, *298*, 869.

(31) Proniewicz, L. M.; Golus, J.; Majcherczyk, H.; Bajdor, K.; Kincaid, J. R. *J. Phys. Chem.* **1994**, *98*, 12856.